

UNIVERSIDADE ESTADUAL DE CAMPINAS
SISTEMA DE BIBLIOTECAS DA UNICAMP
REPOSITÓRIO DA PRODUÇÃO CIENTÍFICA E INTELECTUAL DA UNICAMP

Versão do arquivo anexado / Version of attached file:

Versão do Editor / Published Version

Mais informações no site da editora / Further information on publisher's website:

<https://onlinelibrary.wiley.com/toc/16154169/2022/364/23>

DOI: 10.1002/adsc.202201095

Direitos autorais / Publisher's copyright statement:

©2022 by Wiley-VCH. All rights reserved.

DIRETORIA DE TRATAMENTO DA INFORMAÇÃO

Cidade Universitária Zeferino Vaz Barão Geraldo

CEP 13083-970 – Campinas SP

Fone: (19) 3521-6493

<http://www.repositorio.unicamp.br>

 Very Important Publication

Visible Light-Enhanced C–H Amination of Cyclic Ethers with Iminoiodinanes

Igor D. Jurberg,^{a, b,*} Rene A. Nome,^a Stefano Crespi,^c Teresa D. Z. Atvars,^a and Burkhard König^{b,*}

^a Institute of Chemistry, State University of Campinas, 13083-862, Campinas, SP, Brazil

E-mail: ijurberg@unicamp.br

^b Institute of Organic Chemistry, University of Regensburg, 93053, Regensburg, Germany

E-mail: burkhard.koenig@chemie.uni-regensburg.de

^c Department of Chemistry – Ångström Laboratory, Uppsala University, 75120, Uppsala, Sweden

Manuscript received: October 6, 2022; Revised manuscript received: October 31, 2022;

Version of record online: November 23, 2022



Supporting information for this article is available on the WWW under <https://doi.org/10.1002/adsc.202201095>

© 2022 The Authors. Advanced Synthesis & Catalysis published by Wiley-VCH GmbH. This is an open access article under the terms of the Creative Commons Attribution License, which permits use, distribution and reproduction in any medium, provided the original work is properly cited.

Abstract: A two-step protocol allowing the C–H amination of cyclic ethers with iminoiodinanes, followed by the reduction of the resulting intermediate has been developed for the preparation of amino alcohols. The initial C–H functionalization is accelerated by visible light, improving the reactivity compared to the thermal process performed in the dark. The effect of different substituents on the photochemical reactivity of iminoiodinanes has been studied both experimentally and computationally. Photophysical measurements and DFT calculations were performed to better understand the observed reactivities and corroborate the proposed mechanistic proposal.

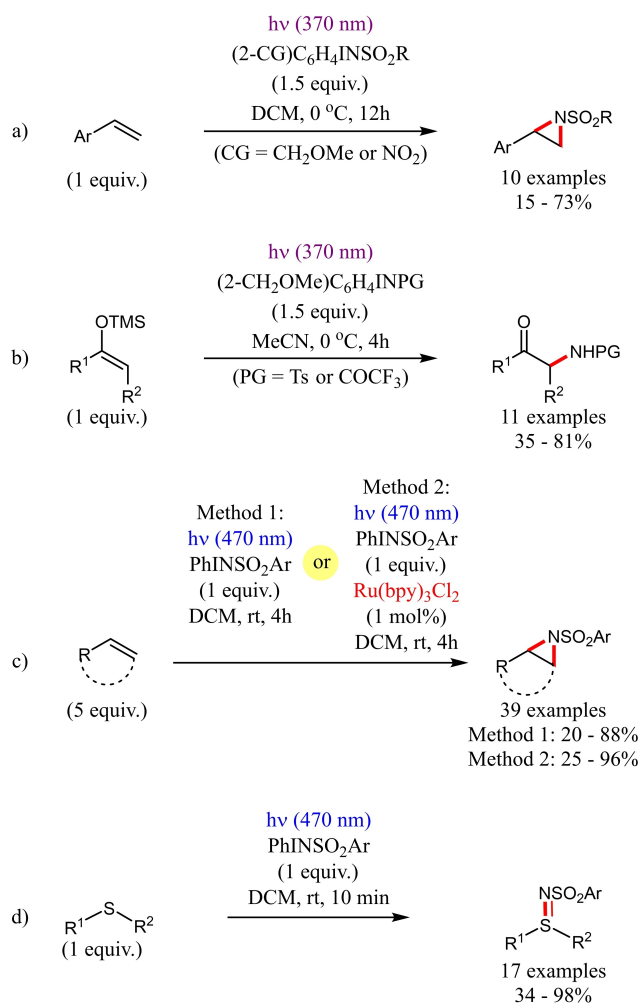
Keywords: Iminoiodinanes; Cyclic Ethers; C–H functionalization; Amino Alcohols; Visible Light; Photochemistry

C–H functionalization strategies have evolved over the past decades into an important research area driven by the ubiquity of C–H bonds in organic molecules and the power of such approaches to streamline the preparation of sophisticated synthetic targets with good selectivity and efficiency.

Among these strategies, C–H aminations are particularly important,^[1–3] as they give access to high-value chemicals from readily available hydrocarbons. Histor-

ically, metal-catalyzed nitrene transfer approaches were the typical choices for such chemical transformations. Remarkable examples involve the Rh-catalyzed preparation of unadorned aziridines from olefins by Ess, Kürti, Falck and co-workers,^[2a] the C–H amination of different arenes, as reported by Falck and co-workers,^[2b] and the C–H amination of numerous complex natural products, as reported by Du Bois and co-workers,^[2c] among many others, including also the use of other metal catalysts^[2d–f] or metal-free conditions.^[3]

In the past decade, the promotion of chemical reactions by visible light irradiation has been established as a powerful technique. Because most organic molecules do not absorb in the visible region, photocatalysts are generally required for initiating electron^[4] or energy transfer events,^[5] which can trigger radical reactions. In contrast to these reaction manifolds, it has been recently reported that some diazo compounds can absorb in the visible region, thus undergoing photolysis to generate free carbenes.^[6] Remarkably, in this same context, iminoiodinanes were also reported to absorb in or close to the visible light region and undergo photolysis to generate highly reactive free nitrene intermediates.^[7] Indeed, Takemoto and co-workers have shown that such *ortho*-stabilized hypervalent iodine compounds can be irradiated under low-energy UV light (black light, 370 nm) to promote the aziridination of olefins (Scheme 1a)^[7a] and the α -amination of silyl enol ethers (Scheme 1b).^[7b] Koenigs and co-workers demonstrated that iminoiodinanes can



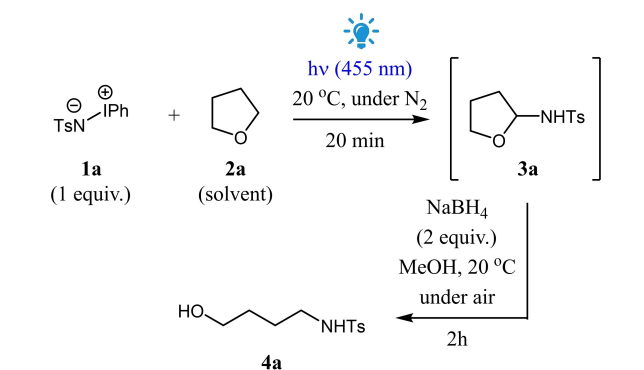
Scheme 1. Representative low-energy light-mediated nitrene transfer reactions using iminoiodinanes. (CG: coordinating group, PG: protecting group)

be irradiated by blue light (470 nm) to enhance the generation of free nitrene intermediates, which were successfully trapped with olefins to afford aziridines (Scheme 1c),^[7c] or with sulfides to generate sulfoxides (Scheme 1d).^[7d]

Building on our own work in visible light-mediated transformations,^[8,9] we became interested in developing visible light-mediated C–H amination reactions using iminoiodinanes **1**. In this context, we started our investigations by studying the reaction between iminoiodinane PhINTs **1a** and THF **2a** under blue light irradiation, aiming at synthesizing the corresponding *N,O*-acetal **3a** as our model reaction^[10] (Table 1).

The desired compound **3a** was successfully observed in the ¹H NMR of the crude reaction mixture, but our attempts to isolate it failed. This compound proved to be unstable, leading to the elimination of TsNH₂ under different purification conditions. Consequently, we decided to reduce it *in situ* using NaBH₄

Table 1. Optimization studies for the C–H amination of THF **2a** using iminoiodinane **1a** under blue light irradiation.



Entry	deviation from optimal conditions	yield (%) ^[a] 4a
1	none	71/70 ^[b]
2	60 °C	60
3	Ru(bpy) ₃ Cl ₂ (1 mol%), 4 h	70
4	Ru(bpy) ₃ Cl ₂ (3 mol%), 4 h	70
5	4-CzIPN (1 mol%), 4 h	67
6	ambient light, under air, 20 °C, 1 h	71
7	ambient light, under air, 60 °C, 1 h	60

^[a] Estimated by ¹H NMR of the crude reaction mixture using 1,3,5-trimethoxybenzene as internal reference.

^[b] Isolated yield.

to afford the corresponding amino alcohol **4a**^[11] (Table 1). When the reaction was performed using THF **2a** as the solvent under blue light irradiation (blue LEDs, 455 nm) at room temperature, we observed the rapid consumption of the iminoiodinane **1a** to afford the *N,O*-acetal **3a** in only 20 min, which upon subsequent addition of NaBH₄ and MeOH led to the formation of amino alcohol **4a** in overall 71% yield (Entry 1, Table 1). Then, we became interested on the possibility of observing a positive effect on the reaction yield of **4a** due to simultaneous blue light irradiation and heating (60 °C) during the first step. However, we only observed a slightly reduced yield of **4a** of 60% (Entry 2, Table 1). Attempts to promote the reaction in the presence of a photoredox catalyst, such as Ru(bpy)₃Cl₂ in different loadings (Entries 3 and 4, Table 1) or 4CzIPN (Entry 5, Table 1) did not afford improved yields for the amino alcohol **4a**. The control experiment of this model reaction under air and ambient light, at 20 °C revealed that this reaction could be also performed with the same high efficiency as previously found under blue light irradiation, (*i.e.* producing **4a** in 71%), but the reaction required a longer reaction time for completion, 1 h^[12] (Entry 6, Table 1). When the reaction is only thermally promoted (heating at 60 °C), a 60% yield for **4a** is again obtained (Entry 7, Table 1).

Based on these optimization studies, we noted the beneficial effect of the blue light irradiation, which

accelerated the first step of our reaction sequence, even if the final yield of the photochemical sequence was found to be the same as the one from the thermal, dark reaction.

At this moment, we hypothesized that no significant alteration in reaction efficiency (*i.e.* chemical yield) was noted because THF **2a** was employed as solvent. However, more important differences in reaction performance could possibly emerge if more valuable cyclic ethers **2** were to be reacted in lower relative amounts with different iminoiodinanes **1**.

With this in mind, we moved forward to evaluate the substrate scope of this transformation under blue light irradiation, while comparing the observed performance with the same reactions under the thermal condition. For this study, the first photochemical (or thermal) step was allowed to run overnight (typically 12 h) for convenience and to ensure full conversion, regardless of the substitution pattern of the reacting partners. Indeed, no negative effects on the obtained yields for the target compounds **4** were noted when comparing longer reaction times with shorter reaction durations showing full conversion (Scheme 2).

Initial investigations using THF **2a** as solvent and different iminoiodinanes PhINSO₂Ar **1** as limiting reagent showed a good general reactivity in most cases, allowing the preparation of amino alcohols **4b** (46%), **4c** (50%), **4d** (70%) and **4e** (71%) in synthetically useful yields. Among these examples, only **4e** could be also prepared with the same efficiency under thermal conditions, 71%. All other amino alcohols **4b**, **4c** and **4d** exhibited significantly lower conversions under ambient light and under air, 30%, 27% and 12%, respectively. In this context, **4d** could be also photochemically accessed in a preparative 1 mmol-scale in a slightly lower 58% yield (see the SI for details). On the other hand, amino alcohol **4f** could not be prepared, presumably due to the very poor solubility of the required iminoiodinane **1f** (Scheme 2). Furthermore, the reaction of 2-methyltetrahydrofuran **2b** used as solvent with PhINTs **1a** afforded a 1:2 mixture of regioisomers **4g**:**4g'** in a combined 66% yield, which was the same outcome produced when the reaction was performed under thermal condition (Scheme 2).

The ring-opening of other common cyclic ethers, such as 1,4-dioxane **2c** or tetrahydropyran (THP) **2d**, both employed as solvents, was more efficient when light irradiation was performed simultaneously with heating to 60 °C, thus affording the corresponding products, **4h** and **4i**, in 23% and 46% isolated yields, respectively. Notably, again, no changes in reaction performance were observed when these transformations were conducted in the presence of photoredox catalysts Ru(bpy)₃Cl₂ and 4-CzIPN; and both products could not be accessed in any extension when the reactions were performed under thermal conditions (Scheme 2). Finally, investigations under photochem-

ical conditions aiming at the ring-opening of phthalan **2j**, xanthene **2k** and (–)-ambroxide **2l** as limiting reagents, in the presence of an excess of iminoiodinane PhINTs **1a** (3 equiv.) allowed synthetically useful yields for the corresponding products **4j** (62%), **4k** (72%) and **4l** (34%),^[13] respectively; while significantly lower yields were obtained for the same reactions performed under thermal conditions (Scheme 2). Remarkably, during our attempts to synthesize **4k**, we observed the possibility of accessing imine derivative **4k'** as the major compound derived from the first step of this reaction sequence, albeit it could be isolated only in a modest yield of 34% (Scheme 2). In this case, this finding suggests that **4k'** is the intermediate that is reduced by NaBH₄ to afford **4k**.

Additionally, attempts aiming at the C–H amination of more functionalized cyclic ethers or containing less reactive α -C–H bonds (*i.e.* more hindered, more geometrically constrained or not benzylic) were unsuccessful (Figure 1).

Based on the observed reactivity of the previously investigated iminoiodinanes **1a–1e**, we became interested in evaluating their photophysical properties and measured UV-Vis absorbance spectra (Figure 2).

Although all iminoiodinanes were initially poorly soluble in DCM or THF (thus typically producing suspensions at 0.05 M concentrations); when the transformations progressed, all productive reaction mixtures became homogeneous, thus showcasing the full con-

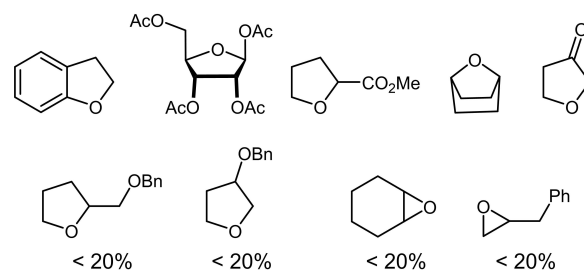


Figure 1. Cyclic ethers that were not successfully C–H aminated under our photochemical conditions.

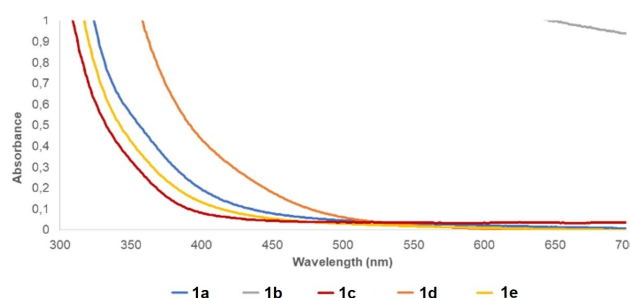
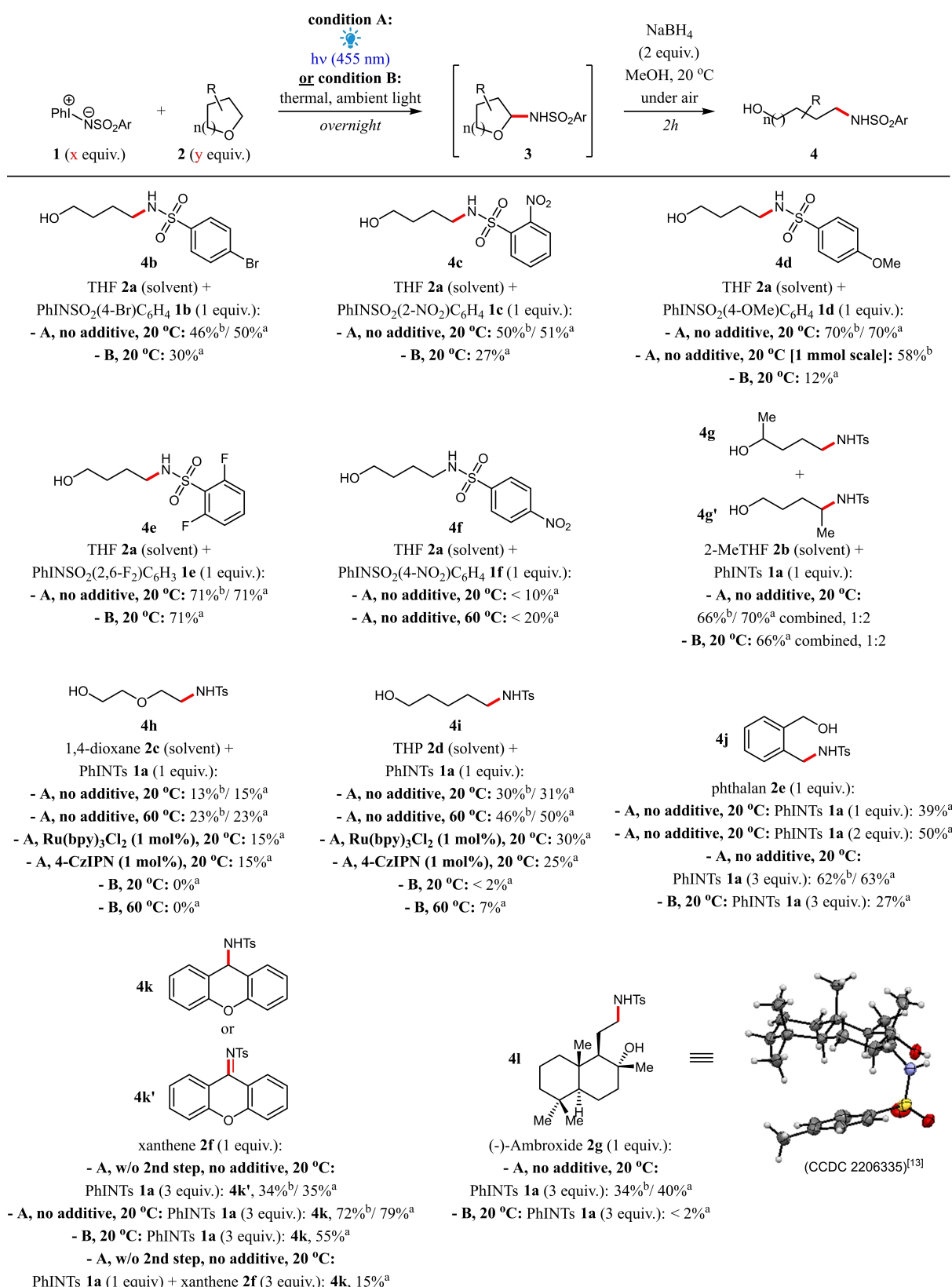


Figure 2. UV-Vis absorbance spectra of iminoiodinanes **1 a–1 e**, 0.001 M in DCM.



Scheme 2. Substrate scope evaluated for the C–H amination/ reduction sequence using different reaction conditions. Reactions were performed at 0.1 mmol-scale of the limiting reagent. **Condition A:** Under N₂, photoirradiated at 455 nm (blue light). **Condition B:** Under air and ambient light, thermally promoted. (In this case, the reaction is not irradiated under blue light). ^aEstimated yield based on ¹H NMR of the crude reaction mixture using 1,3,5-trimethoxybenzene as internal standard. ^bIsolated yield.

sumption of the starting iminoiodinane. In order to prepare homogeneous solutions upon immediate mixing within DCM for the appropriate UV-Vis measurements, diluted mixtures (0.001 M) were prepared. All iminoiodinanes were soluble in DCM in this concentration, except for **1b** (i.e. **1a**, **1c–1e**). Among these substrates, iminoiodinane **1d** showed the strongest bathochromic shift (Figure 2).

Remarkably, in agreement with this observation, iminoiodinane **1d** exhibited the greatest difference in reaction efficiency between the photochemical and the thermal C–H amination reactions leading to amino alcohol **4d**.

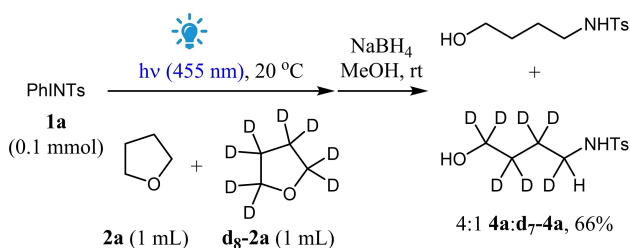
Additional investigation of the reaction mechanism involving the blue light irradiation of iminoiodinane **1a** within a 1:1 mixture of THF: d_8 -THF afforded a 4:1 mixture of **4a**:**d₇-4a** in 66% combined yield, thus revealing a rough estimation of a KIE ≈ 4 (Scheme 3).

This outcome indicates that the C–H breaking event is the rate-determining step (rds) of this transformation.

Then, we became interested in investigating the reactivity of the iminoiodinane **1a** using spectroscopic techniques (see also the SI for additional details). We initially focused our attention on the analysis of UV-Vis spectra of **1a** in DCM as a function of its

concentration. From this data, we calculated the molar extinction coefficient as a function of wavelength (Figure 3, black curve). Overall, from the concentration-dependent absorption spectra, the experimental values of the molar extinction coefficient at 350 nm and 450 nm were in good agreement with the quantum chemical calculations for iminoiodinanes **1a–1e** (see DFT calculations below). In particular, the weak absorption at 450 nm is consistent with a $S_0 \rightarrow T_1$ transition and spin-orbit coupling (SOC), which is enhanced by the presence of a heavy-atom (iodine) in the molecular structure of iminoiodinanes.^[14,15] Then, we measured the emission spectra ($\lambda_{\text{exc}} = 440$ nm) of **1a** in the solid state at $T = 294$ K and 11 K (Figure 3, blue and green curves, respectively). At 294 K, an emission band with broad, structureless and low intensity is centred at 546 nm; whereas at 11 K, an emission band is centred at 633 nm. Furthermore, the measured time-resolved emission decays were approximately 20 ns at 546 nm, at $T = 294$ K; and 60 μ s at 633 nm, at $T = 11$ K (See also Figures S3 and S4 in the SI). Thus, we tentatively assign these two emission bands to the decays from the singlet S_1 and triplet T_1 states, respectively.^[16]

To characterize the effect of the irradiation (using a laser with a similar wavelength of 440 nm) of **1a** in DCM and THF, we measured emission spectra as a function of time over the course of the reaction (approximately for 40 minutes). Figure 4 shows the area-normalized emission spectra as a function of irradiation time. The arrows indicate increasing emission intensity around 503 nm, concomitant with decreasing intensity around 550 nm, and an isosbestic point around 520 nm that is indicative of interconversion between singlet and triplet nitrenes (see Figures S6 and S7 in the SI for a correlation analysis of the data shown in Figure 4). The opposite trend is observed upon irradiation of **1a** in THF, that is, decreasing emission intensity at 503 nm and increasing intensity in the shoulder near 550 nm. We also note that the emission signal registered at 503 nm is coupled to a vibrational transition at 2890 cm^{-1} , which can be presumably assigned to a C–H stretching transition. The lifetime of the nitrene species (major form as



Scheme 3. Investigation of reaction mechanism, KIE.

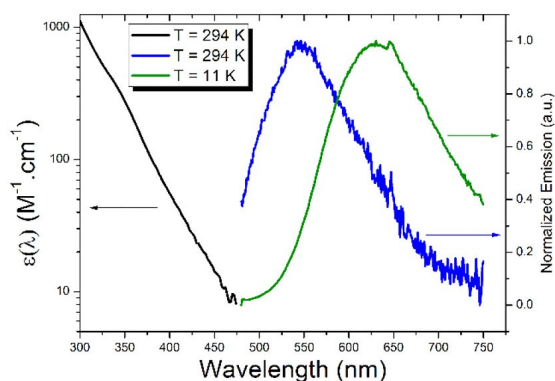


Figure 3. Steady-state electronic spectroscopy. Molar extinction coefficient (black curve) as a function of wavelength for iminoiodinane **1a** in DCM ($[1a] = 1\text{ mmol L}^{-1}$) at $T = 294$ K. Emission of **1a** in the solid state at $T = 294$ K (blue curve) and $T = 11$ K (green curve). $\lambda_{\text{exc}} = 450$ nm.

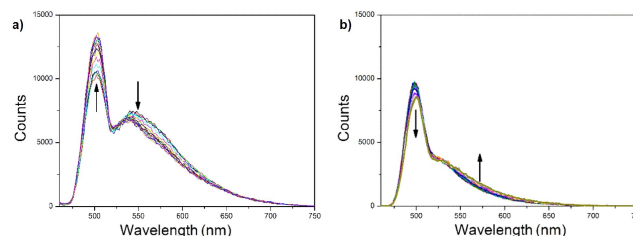


Figure 4. Time-resolved, area-normalized emission spectra of **1a** upon irradiation, a) in DCM and b) in THF. In both cases, $\lambda_{\text{exc}} = 440$ nm and $[1a] = 1\text{ mmol L}^{-1}$.

singlet) in THF, observed at 500 nm, can be estimated to be *ca.* 5 ns (Figure S5).

The difference in behaviour observed in these two solvents can be roughly and tentatively attributed to differences in kinetics between the events associated to the interconversion between singlet and triplet nitrenes.

At this point, we performed computational analyses to optimize the structures of the substituted iminoiodinanes **1a–1e**, and to compare the effect of the substituents on the UV-Vis spectra and on the structure of the triplet states (See SI for details). Natural transition orbital analysis was used to better represent the nature of the first electronic transition. In all cases, the transition primarily involves the excitation from a lone pair on the nitrogen to the N–I σ^* orbital, making this an $n\text{-}\sigma^*$ excitation, in accordance with the previous report from Koenigs and co-workers.^[7c] The oscillator strengths (*f*) are compatible with a non-allowed electronic transition (Table 2). The substituents on the iminoiodinanes **1a–1e** minimally affect the energy of the transition, with the larger effect attributable to the 2-NO₂ group in **1c**. As observed experimentally, more electron-donating groups shift the first electronic

transition bathochromically (Table 2). In addition, more electron-donating groups display longer N–I bond lengths and lower Mulliken spin densities on the iodine, with the notable exception of Br in **1b**, that in the triplet state shows a geometry and spin distribution similar to the tosyl derivative **1a** (Table 2).

The limited effect of the substituents can be attributed to the fact that the orbitals involved in the excitation are not directly conjugated with the aromatic ring. Nevertheless, in the natural transition orbitals (NTO), it is possible to appreciate the contribution of the substituents, which possibly lower (electron-withdrawing groups) or raise (electron donating) the energy of the *n* filled orbital, varying as a consequence the *S*₀–*S*₁ energy gap (Figure 5a). Interestingly, similar effects can be seen in the structure of the triplet states (optimized at the *r*²SCAN-3c level), where the N–I elongates, forming iodobenzene interacting with the triplet nitrene (Figure 5b).

Based on the experimental evidence collected, our mechanistic proposal for this reaction sequence leading to amino alcohols **4** starts with the blue light-accelerated extrusion of PhI from iminoiodinane **1** to afford a nitrene intermediate **5**. Irradiation of **1** may either lead to a singlet nitrene (**5**¹, via *S*₀→*S*₁) or a triplet nitrene (**5**³, via *S*₀→*T*₁). This second hypothesis was confirmed by computing the SOC corrected absorption spectra of the compounds using zero-order regular approximation (ZORA)^[17] and its required basis set (see SI): in all cases, the direct excitation *S*₀→*T*₁ has oscillator strengths in the same order of magnitude as *S*₀→*S*₁, albeit slightly lower in intensity (see Table S1). Moreover, both species can possibly interconvert via inter-system-crossing (ISC, *S*₁→*T*₁) and via reverse intersystem-crossing (RISC, possibly *T*_n or *T*₁→*S*₁).^[18] The SOC values for the *S*₁→*T*₁ conversion at the ground state geometry are: 4-NO₂, **1f** (23 cm^{−1}) > 2,2'-F₂, **1e** (22.7 cm^{−1}) > 4-Br, **1b** (18 cm^{−1}) > 4-Me, **1a** (15 cm^{−1}) > 4-MeO, **1d** (14 cm^{−1}).

Singlet nitrenes **5**¹ can presumably undergo direct C–H insertion to provide the *N,O*-acetal intermediate **3**, while triplet nitrenes **5**³ can undergo hydrogen atom transfer (HAT) with the cyclic ether **2**, followed by radical combination to afford the corresponding *N,O*-acetal **3**. Upon addition of NaBH₄, this intermediate is reduced to the observed amino alcohol **4** (Scheme 4).

In summary, we have studied a blue light-enhanced C–H amination strategy of cyclic ethers employing iminoiodinanes, followed by a NaBH₄-reduction event leading to the corresponding amino alcohols. Yields in the range 23–72% were obtained for activated cyclic ethers reacting with different iminoiodinanes, while other cyclic ethers showed to be less reactive. Key elements of the reaction mechanism were proposed based on experimental evidence, spectroscopic analyses and DFT calculations. Of note, we showed that the

Table 2. Simulated properties of the *S*₀→*S*₁ transition and of the excited triplet states of different iminoiodinanes **1a–1e** at the CPCM(DCM)-TD-M06-2X-D3/def2-TZVPD//*r*²SCAN-3c level.

	Ground state (<i>S</i> ₀)		Triplet state (<i>T</i> ₁)		
	λ (nm)	<i>f</i>	N–I (Å)	Spin density (N)	Spin density (I)
(1a) 4-Me	362.1	6.05E-03	3.189	1.71	0.12
(1b) 4-Br	359.9	6.85E-03	3.118	1.70	0.15
(1c) 2-NO ₂	349.1	5.91E-03	2.820	1.55	0.28
(1d) 4-MeO	365.3	6.17E-03	3.218	1.67	0.10
(1e) 2,2'-F ₂	360.9	6.70E-03	2.824	1.56	0.28

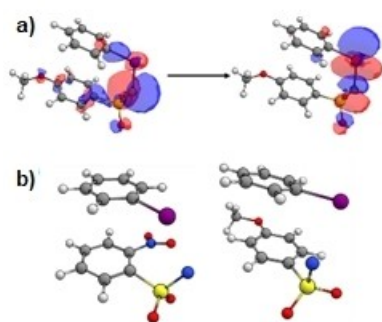
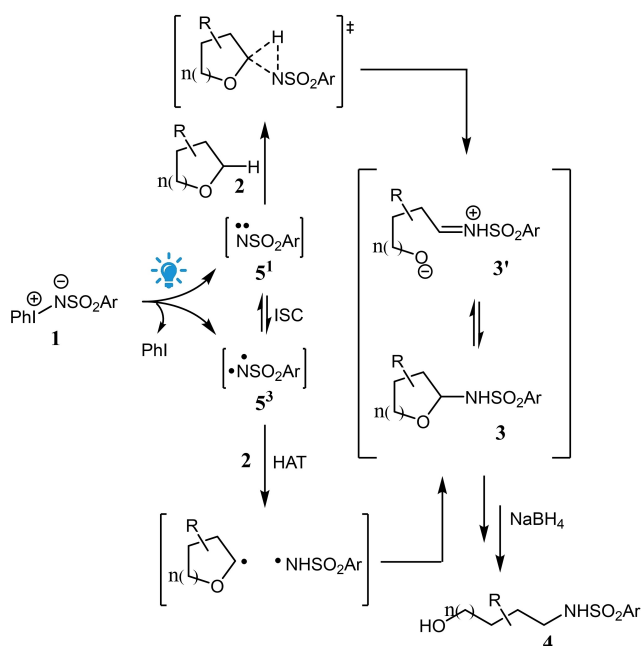


Figure 5. a) Natural transition orbitals (NTO) associated with the predominant component found in the first singlet electronic transition of (4-MeO)C₆H₄SO₂NIPh. b) Structures of (2-NO₂)C₆H₄SO₂NIPh and (4-MeO)C₆H₄SO₂NIPh in their triplet states.



Scheme 4. Proposed reaction mechanism.

iminoiodinane **1d** carrying a *para*-substituted electron-donor group (OMe) shows a stronger bathochromic shift in comparison to the other evaluated iminoiodinanes **1**, which correlates with the improvement observed in reaction yield for amino alcohol **4d** using the photochemical process (70%) in regard to the thermal, dark reaction (12%). Finally, spectroscopic measurements and calculations indicate that singlet and triplet nitrenes are involved as key intermediates in the first step of this reaction sequence; and an overall mechanistic view has been proposed.

Experimental Section

General Experimental Procedure for the Preparation of Amino Alcohols **4** Using the Cyclic Ether **2** as Solvent

Under air, at rt, a 5-mL crimp cap vial containing a stirring bar is charged with iminoiodinane **1** (1 equiv.) and the cyclic ether **2** (1 or 2 mL). Then, the vial is closed and the reaction mixture is degassed via freeze-pump-thaw (3×), being back-filled with N₂ and irradiated under blue light (455 nm) overnight, while the temperature is controlled at 20°C or 60°C using a thermostatic bath. Then, the reaction vial is opened to air, NaBH₄ (2 equiv.) and MeOH (1 mL) are sequentially added and the reaction mixture is allowed to stir under air at rt for additional 2 h. Then, water is added, and the resulting mixture is extracted with AcOEt (3×). The combined organic phases are dried (MgSO₄), filtered and concentrated under reduced pressure. The resulting residue is purified by flash column chromatography to afford the corresponding amino alcohol **4** in the stated yield.

General Experimental Procedure for the Preparation of Amino Alcohols **4** Using the Cyclic Ether **2** as Limiting Reagent

Under air, at rt, a 5-mL crimp cap vial containing a stirring bar is charged with the cyclic ether **2** (1 equiv.), DCM (2 mL) and the iminoiodinane **1** (3 equiv.). Then, the vial is closed, and the reaction mixture is degassed via freeze-pump-thaw (3×), being back-filled with N₂ and irradiated under blue light (455 nm) overnight, while the temperature is controlled at 20°C using a thermostatic bath. Then, the reaction vial is opened to air, NaBH₄ (2 equiv.) and MeOH (1 mL) are sequentially added, and the reaction mixture is allowed to stir under air at rt for additional 2 h. Then, water is added, and the resulting mixture is extracted with AcOEt (3×). The combined organic phases are dried (MgSO₄), filtered and concentrated under reduced pressure. The resulting residue is purified by flash column chromatography to afford the corresponding amino alcohol **4** in the stated yield.

Acknowledgements

IDJ greatly acknowledges a Visiting Scholar Fellowship from CAPES (88881.512988/2020-01) – Alexander von Humboldt Foundation (1144417-BRA-HFSTCAPES-E). Fapesp is also greatly acknowledged for Regular Research Grants to IDJ (2019/01235-8), RAN (2020/10541-2) and TDZA (2009/14153-8). SC thanks the Swedish Vetenskapsrådet for a Starting Grant (2021-05414). The project was partially funded by the Deutsche Forschungsgemeinschaft (DFG, German Research Foundation) TRR 325 444632635. The authors thank Sérgio Coelho and Milene Martins (both from Unicamp, Brazil) for the measurements shown in Figures 3 and S3.

References

- [1] For a selection of reviews, see: a) Y. Park, Y. Kim, S. Chang, *Chem. Rev.* **2017**, *117*, 9247–9301; b) D. Hazeldar, P.-A. Nocquet, P. Compain, *Org. Chem. Front.* **2017**, *4*, 2500–2521; c) M. Ju, J. M. Schomaker, *Nature Rev. Chem.* **2021**, *5*, 580–594; d) J. Du Bois, *Org. Process Res. Dev.* **2011**, *15*, 758–762; e) J. L. Roizen, M. E. Harvey, J. Du Bois, *Acc. Chem. Res.* **2012**, *45*, 911–922.
- [2] For a selection of metal-catalyzed approaches, see: a) J. L. Jat, M. P. Paudyal, H. Gao, Q.-L. Xu, M. Yousufuddin, D. Devarajan, D. H. Ess, L. Kürti, J. R. Falck, *Science* **2014**, *343*, 61–65; b) M. P. Paudyal, A. M. Adebesein, S. R. Burt, D. H. Ess, Z. Ma, L. Kürti, J. R. Falck, *Science* **2016**, *353*, 1144–1147; c) N. D. Chiappini, J. B. C. Mack, J. Du Bois, *Angew. Chem. Int. Ed.* **2018**, *57*, 4956–4959; d) M. R. Fructos, S. Trofimenko, M. M. Díaz-Requejo, P. J. Pérez, *J. Am. Chem. Soc.* **2006**, *128*, 11784–11791; e) Z. Li, D. A. Capretto, R. Rahaman, C. He, *Angew. Chem. Int. Ed.* **2007**, *46*, 5184–5186; f) V. Bagchi, P. Paraskevopoulou, P. Das, L. Chi, Q. Wang, A. Choudhury, J. S. Mathieson, L. Cronin, D. B. Pardue, T. R. Cundari, G. Mitrikas, Y. Sanakis, P.

- Stavropoulos, *J. Am. Chem. Soc.* **2014**, *136*, 11362–11381.
- [3] For a selection of metal-free approaches, see: a) K. Kiyokawa, T. Kosaka, S. Minakata, *Org. Lett.* **2013**, *15*, 4858–4861; b) J. Li, P. W. H. Chan, C.-M. Che, *Org. Lett.* **2005**, *7*, 5801–5804; c) M. Ochiai, K. Miyamoto, T. Kaneaki, S. Hayashi, W. Nakanishi, *Science* **2011**, *332*, 448–451.
- [4] For representative reviews, see: a) C. K. Prier, D. A. Rankic, D. W. C. MacMillan, *Chem. Rev.* **2013**, *113*, 5322–5363; b) N. A. Romero, D. A. Nicewicz, *Chem. Rev.* **2016**, *116*, 10075–10166; c) I. Ghosh, L. Marzo, A. Das, R. Shaikh, B. König, *Acc. Chem. Res.* **2016**, *49*, 1566–1577.
- [5] For representative reviews, see: a) F. Strieth-Kalthoff, M. J. James, M. Teders, L. Pitzer, F. Glorius, *Chem. Soc. Rev.* **2018**, *47*, 7190–7202; b) F. Strieth-Kalthoff, F. Glorius, *Chem.* **2020**, *6*, 1888–1903.
- [6] For a selection of representative references, see: a) I. D. Jurberg, H. W. L. Davies, *Chem. Sci.* **2018**, *9*, 5112–5118; b) Z. Yang, M. L. Stivanin, I. D. Jurberg, R. M. Koenigs, *Chem. Soc. Rev.* **2020**, *49*, 6833–6847; c) J. Durka, J. Turkowska, D. Gryko, *ACS Sustainable Chem. Eng.* **2021**, *9*, 8895–8918.
- [7] a) S. Masakado, Y. Kobayashi, Y. Takemoto, *Chem. Pharm. Bull.* **2018**, *66*, 688–690; b) Y. Kobayashi, S. Masakado, Y. Takemoto, *Angew. Chem. Int. Ed.* **2018**, *57*, 693–697; c) Y. Guo, C. Pei, R. M. Koenigs, *Nat. Commun.* **2022**, *13*, DOI 1038/s41467-021-27687-6; d) Y. Guo, C. Pei, C. Empel, S. Jana, R. M. Koenigs, *ChemPhotoChem* **2022**, *6*, e202100293.
- [8] For recent contributions from the Jurberg group, see: a) A. F. da Silva, M. A. S. Afonso, R. A. Cormanich, I. D. Jurberg, *Chem. Eur. J.* **2020**, *26*, 5648–5653; b) R. D. C. Gallo, M. Duarte, A. F. da Silva, C. Y. Okada Jr, V. M. Deflon, I. D. Jurberg, *Org. Lett.* **2021**, *23*, 8916–8920; c) L. S. Munaretto, C. Y. dos Santos, R. D. C. Gallo, C. Y. Okada Jr., V. M. Deflon, I. D. Jurberg, *Org. Lett.* **2021**, *23*, 9292–9296; d) C. Y. Okada, Jr, C. Y. dos Santos, I. D. Jurberg, *Tetrahedron* **2020**, *76*, 131316.
- [9] For recent contributions from the König group, see: a) K. Murugesan, K. Donabauer, R. Narobe, V. Derdau, A. Bauer, B. König, *ACS Catal.* **2022**, *12*, 3974–3984; b) R. Narobe, K. Murugesan, S. Schmid, B. König, *ACS Catal.* **2022**, *12*, 809–817; c) R. Narobe, K. Murugesan, C. Haag, T. E. Schirmer, B. König, *Chem. Commun.* **2022**, *58*, 8778–8781; d) K. Murugesan, K. Donabauer, B. König, *Angew. Chem. Int. Ed.* **2021**, *60*, 2439–2445.
- [10] For previous examples of representative C–H amination methods of cyclic ethers, see: a) M. Ochiai, S. Yamane, M. M. Hoque, M. Saito, K. Miyamoto, *Chem. Commun.* **2012**, *48*, 5280–5282; b) L. He, J. Yu, J. Zhang, X.-Q. Yu, *Org. Lett.* **2007**, *9*, 2277–2280; c) M. R. Fructos, S. Trofimenko, M. M. Díaz-Requejo, P. J. Pérez, *J. Am. Chem. Soc.* **2006**, *128*, 11784–11791; d) J. Campos, S. K. Goforth, R. H. Crabtree, T. B. Gunnoe, *RSC Adv.* **2014**, *4*, 47951–47957.
- [11] Although this reaction sequence is not redox-economical, it readily leads to easier-to-handle, useful amino alcohols. For other examples of functionalization of *N,O*-acetals, see: a) C. R. Berry, R. P. Hsung, J. E. Antoline, M. E. Petersen, R. Challeppan, J. A. Nielson, *J. Org. Chem.* **2005**, *70*, 4038–4042; b) K. Nishimura, R. Hanzawa, T. Sugai, H. Fuwa, *J. Org. Chem.* **2021**, *86*, 6674–6697.
- [12] This is in agreement with a previous observation. See: C. Tejo, Y. F. A. See, M. Mathiew, P. W. H. Chan, *Org. Biomol. Chem.* **2016**, *14*, 844–848.
- [13] CCDC 2206335 contains the supplementary crystallographic data for this paper. These data can be obtained free of charge from The Cambridge Crystallographic Data Centre via www.ccdc.cam.ac.uk/structures.
- [14] M. Nakajima, S. Nagasawa, K. Matsumoto, T. Kuribara, A. Muranaka, M. Uchiyama, T. Nemoto, *Angew. Chem. Int. Ed.* **2020**, *59*, 6847–6852.
- [15] The involvement of singlet and triplet nitrenes derived from Ar¹INSO₂Ar² has been previously discussed based on DFT calculations. See: B. A. Shainyan, A. V. Kuzmin, *J. Phys. Org. Chem.* **2014**, *27*, 156–162.
- [16] The observed lifetimes for singlet and triplet nitrenes are in good agreement in terms of magnitude with previously reported values. See for instance: J. Kubicki, H. L. Luk, Y. Zhang, S. Vyas, H.-L. Peng, C. M. Hadad, M. S. Platz, *J. Am. Chem. Soc.* **2012**, *134*, 7036–7044.
- [17] E. van Lenthe, J. G. Snijders, E. J. Baerends, *J. Chem. Phys.* **1996**, *105*, 6505–6516.
- [18] For a more detailed discussion on RISC and potential applications in material science, see: a) N. Aizawa, Y. Harabuchi, S. Maeda, Y.-J. Pu, *Nat. Commun.* **2020**, *11*, DOI 10.1038/s41467-020-17777-2; b) M. A. Bryden, E. Zysman-Colman, *Chem. Soc. Rev.* **2021**, *50*, 7587–7680.